CellPress
OPEN ACCESS

Trends in
Chemistry

Review

Van der Waals materials for paper electronics

Wenliang Zhang,[1,2] Kexin He,[3] Andres Castellanos-Gomez,[2,*] and Yong Xie[2,3,*]

Two-dimensional van der Waals (vdW) materials have attracted extensive interest because of their superior electrical, optical, thermodynamic, and mechanical properties, which hold great potential in the development of flexible paper-based devices. The family of vdW materials is significantly diverse and their electronic features range from metallic to semiconducting and superconducting. This review covers the state-of-the-art research progress in the development of various vdW materials from fabrication to applications in paper-based electronics and optoelectronics. In particular, the promising applications of vdW materials integrated with paper as flexible mechanical sensors, environmental sensors, and photodetectors are highlighted. The remaining challenges and prospects related to paper-based devices with vdW materials are discussed. This review provides a comprehensive roadmap to inspire future breakthroughs.

Highlights

2D Two-dimensional van der Waals (vdW) materials feature an extended crystalline planar configuration that is held together by intralayer covalent or ionic bonds, as well as interlayer vdW interactions, which exhibit fascinating electrical, optical, thermal, and mechanical properties.

The family of vdW materials shows remarkable diversity, displays a broad range of electronic properties and chemical composition, and can be integrated on paper through solvent-based and solvent-free techniques.

Paper-based devices using various vdW materials are delivering promising applications in mechanical sensing, environmental monitoring, and optical detection, and will promote the rapid development of flexible electronics and optoelectronics.

Paper electronics with vdW materials

As resource scarcity and environmental pollution caused by electronic waste (e-waste) continues to grow, developing eco-friendly flexible devices from renewable resources to create a sustainable future has attracted extensive attention [1,2]. Cellulose paper, with its abundant raw materials, physical flexibility, biodegradability, and biocompatibility, represents a promising candidate for constructing cost-effective, disposable devices [3–5]. Distinct from traditional glass and plastic substrates, cellulose paper has unique 3D hierarchical architectures, high porosity, large specific surface area, and abundant surface hydroxyl functional groups [6,7]. These features enable paper to function as a flexible building support, namely a scaffold, for the incorporation of diverse conductive or active materials, thus facilitating for the construction of disposable electronic and optoelectronic devices. Paper devices, for instance, can sense water temperature when adhered to a cup, or even detect emotional shifts when placed on the forehead [8]. Functionalized papers also serve as sustainable platforms for energy devices [9,10], biodetection systems [11], and human–machine interfaces [12,13]. Furthermore, paper can be utilized as an electronic component in numerous applications such as paper-based transistors [14] and complementary metal oxide semiconductor (CMOS) devices [9] where it functions as a dielectric.

Despite the widespread employment of conductive materials such as metal nanoparticles and carbon nanotubes as the electrical transport pathways in paper-based circuits [10,11], the urgent need for the next generation of paper-based devices with diverse and fascinating functionalities persists. Since the first isolation of graphene [12], the family of 2D vdW materials has experienced rapid expansion, and various novel features have been explored. Owing to their exceptional electrical, optical, thermodynamic, and mechanical properties, 2D vdW materials hold tremendous promise for applications in flexible electronics and optoelectronics [13,15–18].

Although several recent reviews have documented advances in conductive and functional materials for paper-based devices, including metals, polymers, carbon materials, oxides, and their composites [5,19–21], there is a noticeable gap in the literature on emerging vdW materials.

[1]College of Bioresources Chemical and Materials Engineering, Shaanxi University of Science and Technology, Xi'an 710016, China
[2]Materials Science Factory, Instituto de Ciencia de Materiales de Madrid (ICMM), Consejo Superior de Investigaciones Científicas (CSIC), Madrid E-28049, Spain
[3]School of Advanced Materials and Nanotechnology, Xidian University, Xi'an 710071, China

*Correspondence:
andres.castellanos@csic.es (A. Castellanos-Gomez) and
xieyong.nwpu@gmail.com (Y. Xie).

This review highlights recent advances in paper electronics integrated with vdW materials, as illustrated by the overview in Figure 1. First, the diversity of vdW materials and their fabrication methods on paper are introduced. We then discuss the progress of their application towards electronics, including the development of mechanical sensors, humidity sensors, temperature sensors, and gas sensors. Furthermore, various paper-based photodetectors using vdW materials are reviewed in detail. Finally, challenges and prospects in the thriving field of paper-based devices with vdW materials are addressed.

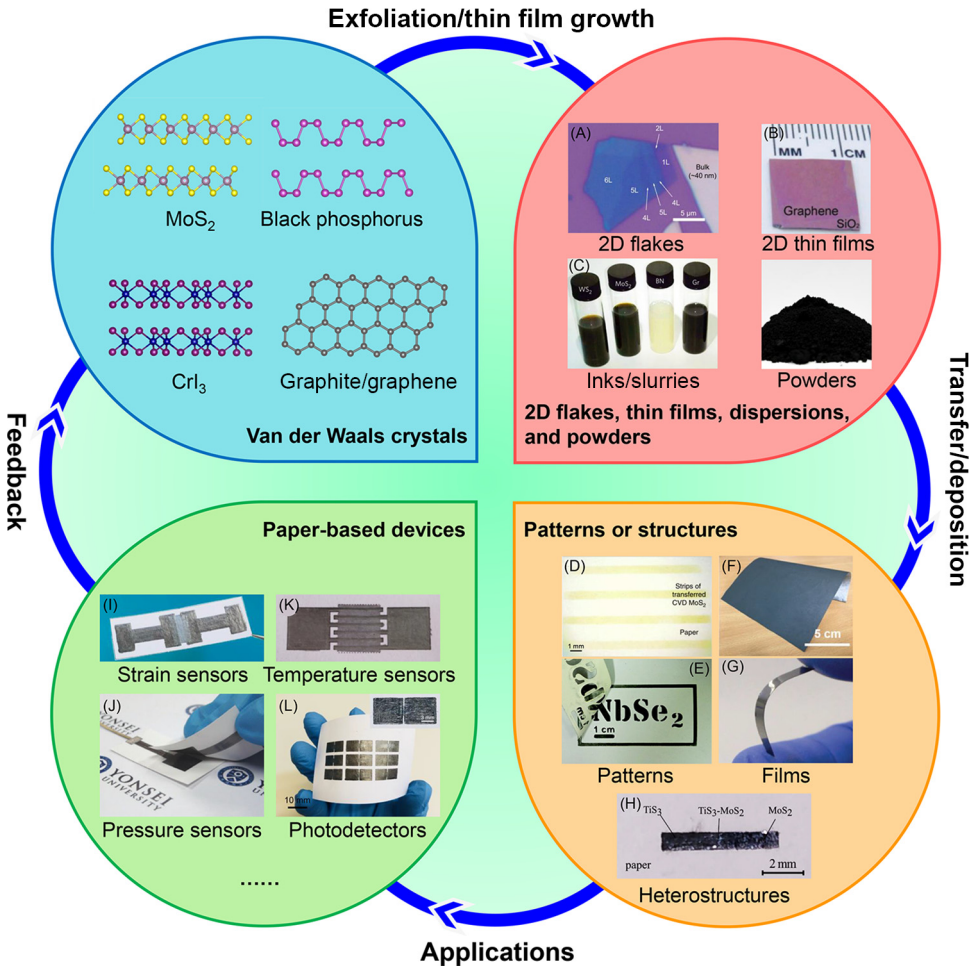

Figure 1. An overview of integration of van der Waals (vdW) materials-based devices on paper. (A) 2D $MoTe_2$ flakes prepared by mechanical exfoliation. Adapted, with permission, from [27]. (B) A 2D graphene thin film grown by the CVD method. Adapted, with permission, from [17]. (C) Water-based 2D crystal inks. Adapted, with permission, from [38]. (D) Strips of transferred CVD MoS_2 on paper. Adapted, with permission, from [35]. (E) A $NbSe_2$ film abrasively deposited on paper following a user-defined pattern. Adapted, with permission, from [34]. (F) A mulberry paper-based graphene film. Adapted, with permission, from [58]. (G) A thick film of chemically exfoliated 1T MoS_2. Adapted, with permission, from [32]. (H) A TiS_3-MoS_2 heterostructure on paper. Adapted, with permission, from [100]. (I) A WS_2 strain sensor on paper. Adapted, with permission, from [65]. (J) A graphite-based capacitive pressure sensor on paper. Adapted, with permission, from [54]. (K) A WS_2 temperature sensor with interdigitated graphite electrodes on paper. Adapted, with permission, from [79]. (L) A WS_2 photodetector array on paper. Adapted, with permission, from [91]. Abbreviations: CVD, chemical vapor deposition; Gr, graphene.

Glossary

Chemical vapor deposition (CVD): a widely used process for creating high-quality thin films and coatings that involves thermally induced chemical reactions of a heated substrate, where reagents are supplied in gaseous form.

Coffee-ring effect: a phenomenon in the process of inkjet printing. Owing to the faster evaporation rate at the edge, printed inks dry unevenly and thus form a non-uniform pattern.

Piezoelectricity: a phenomenon in which some crystalline materials are polarized when subjected to mechanical stress, creating an electric charge at their surface. There is a linear relationship between the mechanical stress applied to a piezoelectric material and the charge it generates, which can be expressed as $Q = d \times F$, where Q is the charge generated, F is the applied mechanical force, and d is the piezoelectric coefficient.

Piezoresistivity: an electromechanical effect characterized by the change in electrical resistivity of a material upon applied mechanical stress. The piezoresistivity phenomenon can be expressed as $\Delta R = R_0 \times \pi \times \sigma$, where ΔR is the change in resistance, R_0 is the initial resistance, π is the piezoresistive coefficient of the material, and σ is the stress applied.

Sensitivity: the sensitivity of strain and pressure sensors is a significant parameter that denotes the relative change in electrical value per strain/pressure unit. For instance, the sensitivities of the piezoresistive pressure sensor (S_p) and strain sensor (S_s) can be defined as $S_p = (\Delta R R0)\Delta P, and S_s = (\Delta R R0)\varepsilon$, respectively, where ΔR is the change in resistance, R_0 is the initial resistance, ΔP is the change in pressure applied, and ε is the change in strain applied.

Transition metal dichalcogenides (TMDCs): a class of 2D materials with a chemical formula of MX_2, where M represents transition metal element (e.g., W, Mo, Ga, In, …) and X is a chalcogen element (S, Se, and Te).

Van der Waals (vdW) interactions: electrostatic forces caused by a temporarily fluctuating dipole moment arising from a brief shift of orbital electrons to one side of an atom or molecule.

Young's modulus: a numerical constant that describes the elastic properties of a material upon unidirectional stretching or compression, which is a measure of the ability of a material to

withstand changes in length when subjected to lengthwise tension or compression.

vdW materials with great potential in paper-based devices

Two-dimensional vdW materials feature an extended crystalline planar configuration that is held together by intralayer covalent or ionic bonds, as well as interlayer **vdW interactions** (see Glossary). As shown in Figure 2A, vdW forces are the weakest intermolecular interaction, with an energy strength in range of ~0.1–10 kJ mol^{-1}, much lower than that of intramolecular ionic and covalent bonds (~100–1000 kJ mol^{-1}), and even intermolecular hydrogen bonds [22]. This phenomenon provides a theoretical foundation for the easy exfoliation of individual layers from bulk materials. Numerous exfoliation strategies have been proposed, including ultrasound-assisted liquid phase exfoliation [23], solvothermal-assisted liquid phase exfoliation [24], electrochemical exfoliation [25], and mechanical exfoliation [26,27].

The family of the 2D vdW materials is significantly diverse, as demonstrated in Figure 2B. These materials cover a broad range of electronic properties, including superconductors, semimetals, semiconductors, wide-gap insulators, and ferromagnets (Figure 2C). They also range from

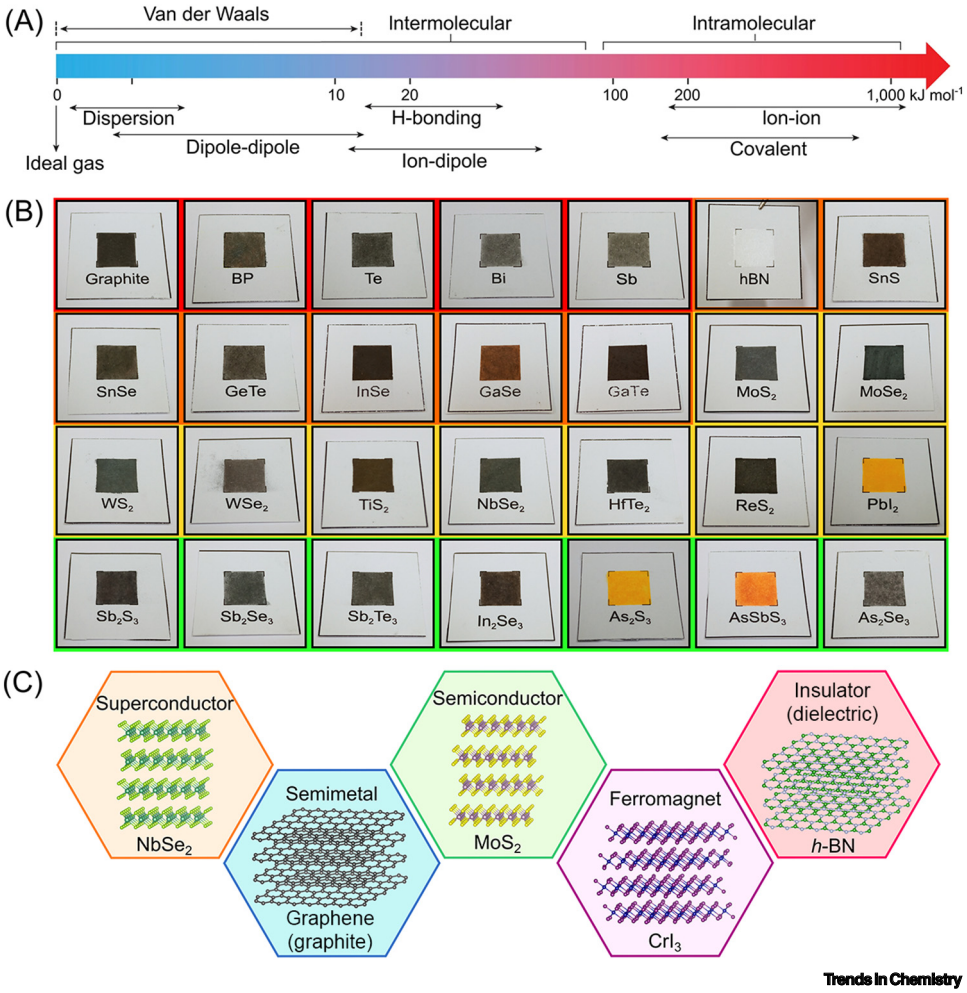

Figure 2. Emerging van der Waals (vdW) materials in paper-based devices. (A) Energies of different molecular interactions including vdW interaction, intermolecular H bonding, intramolecular ion–ion bonding, and covalent bonding. Adapted, with permission, from [22]. (B) Catalog of various vdW films deposited on paper. Adapted, with permission, from [28]. (C) Schematic drawings of the atomic structure of vdW materials with different electronic properties.

single-element materials [e.g., graphene/graphite, black phosphorus (BP), germanene, and tellurium] to multiple-element materials (e.g., $NbSe_2$, WS_2, $MoSe_2$, In_2Se_3, Sb_2Te_3, MoO_3, and $PbSnS_2$) [28]. In research on paper-based devices, graphene/graphite is the most common vdW material. It has often been utilized as the conductive electrode and resistive sensing material for energy harvesting [29], energy storage [30], and sensors [31]. However, a series of 2D vdW materials beyond graphene/graphite have been developed, further expanding their application in paper-based devices. One such emerging class of 2D vdW materials are the **transition metal dichalcogenides (TMDCs)**, which exhibit exceptional properties such as strong light–matter interaction and versatile electronic features ranging from metallic to semiconducting to superconducting [32–34]. Semiconducting TMDC materials have sizeable bandgaps, which complement the gapless graphene and thus could be applied in switching and optoelectronic devices [35,36]. It is believed that these 2D vdW materials hold great potential to aid the development of paper-based electronics and optoelectronics.

Fabrication methods for paper-based devices

Although the distinct properties of cellulose paper, including its pronounced roughness and surface hydroxyl groups, present challenges for conventional microfabrication methods, these characteristics also ensure robust adherence of active materials during device fabrication. The fabrication of paper-based devices can be categorized into solvent-based and solvent-free techniques. Figure 3 schematically illustrates several widely used methods.

Solvent-based fabrication methods

The prevalent solvent-based fabrication processes for paper-based devices involve the dispersion of flakes of van der Waals materials in solvents to form inks and slurries [37]. These can be deposited onto substrates through inkjet printing, spray coating, screen printing, and dip-coating (Figure 3A–D).

Inkjet printing (Figure 3A) is a widespread method because it has a short processing time and is mass-produced [38]. The inkjet printing technology simplifies the precise deposition of different functional materials in a maskless way. However, during inkjet printing, ink rheology must be

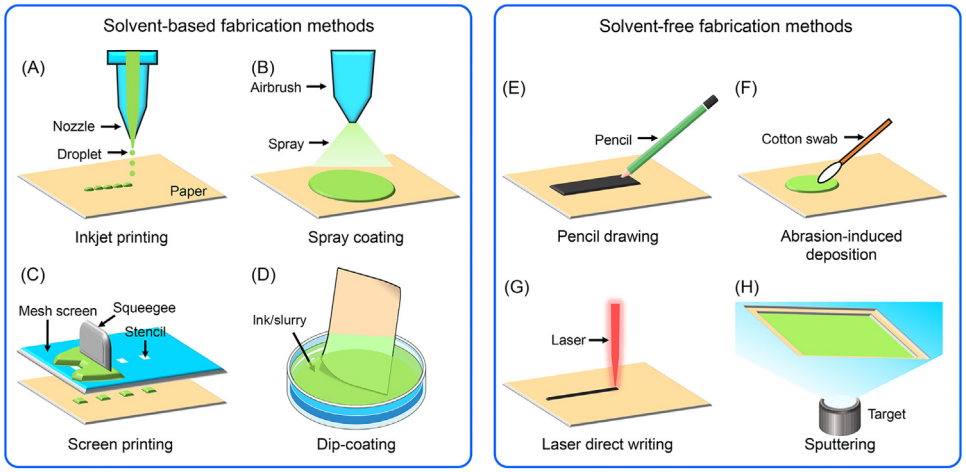

Figure 3. Schematic Illustration of fabrication methods for paper-based devices. (A–D) Solvent-based fabrication methods, including inkjet printing (A), spray coating (B), screen printing (C), and dip-coating (D). (E–H) Solvent-free fabrication methods, including pencil drawing (E), abrasion-induced deposition (F), direct laser writing (G), and sputtering (H).

carefully designed to avoid ink-injector clogging. Common phenomena may affect the printing resolution, including irregular diffusion of the inks on the fibrous paper substrates and the **coffee-ring effect** [39].

Spray coating (Figure 3B) is used to apply ink or paint to the surface of substrates with the aid of air pressure [40]. During the spraying process, air or nitrogen is usually used as a compressed gas to atomize the active particles. Unlike inkjet printing intended for delicate patterns, spray coating is more promising for the manufacture of large-format products.

Screen printing (Figure 3C) operates on the principle that only the graphic mesh part of the printing plate allows the passage of inks [41]. Under the pressing of a squeegee, the inks are transferred to the substrate, thus creating a graphic identical to the original printing plate. The screen printing technique is characterized by strong printing adaptability, high reproducibility, and good stereoscopic effect, and can significantly contribute to the production of low-cost paper-based devices.

Dip-coating (Figure 3D) involves immersing a substrate into liquid phase coating solutions. After withdrawal from the solution tank, the substrate can be fully infiltrated to form a wet coating with a high mass loading [42]. The fibrous and porous structure of paper substrates is particularly conducive to the use of this method to fabricate paper-based devices [43].

Solvent-free fabrication methods

Fabrication in the absence of solvents is desirable to avoid the prolonged high-temperature heat treatment used to evaporate the solvents, and also improves the electrical contact of functional particles or flakes. Several solvent-free fabrication methods are illustrated in Figure 3E–H.

Pencil drawing (Figure 3E) provides a simple and fast way to create graphite traces with arbitrary patterns on paper. The graphite traces can function as conductive electrodes or active elements for paper-based functional devices, and are resistant to oxidation, corrosion, and radiation [44,45].

Abrasion-induced deposition (Figure 3F) is a universally applicable technique that allows the deposition of a wider diversity of layered vdW materials. Similarly to pencil drawing, the friction forces generated between the material and the substrate during the abrasion process are sufficiently powerful to break weak interlayer vdW interactions, leaving a network/film of interconnected flakes [28,46].

Laser direct writing method (Figure 3G) is employed to synthesize and pattern graphene material through the direct conversion of raw materials, where a focused laser beam induces a localized photothermal or photochemical reaction [47]. This method features high resolution, non-contact processing, and eco-friendliness without using masks or toxic chemicals. Notably, cellulose paper can be converted into graphene, which can be used in a vast array of applications such as sensing, energy storage, electrocatalysis, and generators [48–50].

The sputtering method (Figure 3H) has received great attention because of its simplicity and reliability, as well as its ability (and repeatability) to cover large areas [51,52]. The sputtering process is mainly based on bombarding the target material with ions generated by plasma formed during direct current (DC) and radiofrequency (RF) gas discharge.

Integrating vdW materials with paper for mechanical sensor applications

Flexible mechanical sensors have attracted significant interest owing to their sensitive ability to detect strain and pressure. The application of strain or pressure leads to a change in electrical

properties such as resistance and capacitance, and sensing involves transduction mechanisms such as **piezoresistivity** [53], capacitance [54], and **piezoelectricity** [55]. For piezoresistive strain sensors, the sensing function is not only from the intrinsic resistive properties and geometric influences of the materials but also from disconnection of micro/nanomaterials, tunneling effects, and the formation of microcracks within the film [56]. These strain/pressure-sensitive devices are generally composed of sensing materials, supporting substrates, and conductive electrodes, where the first two components play significant roles in the **sensitivity**, dynamic range, flexibility, and stability of the device [57,58]. This section highlights several promising applications of paper-supported devices with vdW materials in mechanical sensing.

Pressure sensors

As shown in Figure 4A, pressure sensors have various configurations, including single-layer, double-layer, and multi-layer. For pressure sensors, the construction of microstructures on substrates is a practical approach for enhancing the performance of the device, such as sensitivity, dynamic range, and durability. Owing to its inherently porous structure and rough surface, cellulose paper promises to be a competitive candidate for the deposition of vdW materials to produce high-performance pressure sensors. A composite paper-based pressure sensor composed of softwood cellulose fibers and graphite nanoplates was fabricated through a papermaking process, and this delivered a wide detection range of up to 1421 kPa [59]. As shown in Figure 4B, upon applying pressure, the electrical resistance of the device changed, which could be attributed to the reduced cross-section of the composite paper. A graphene–paper pressure sensor was developed using a porous tissue paper, and exhibited

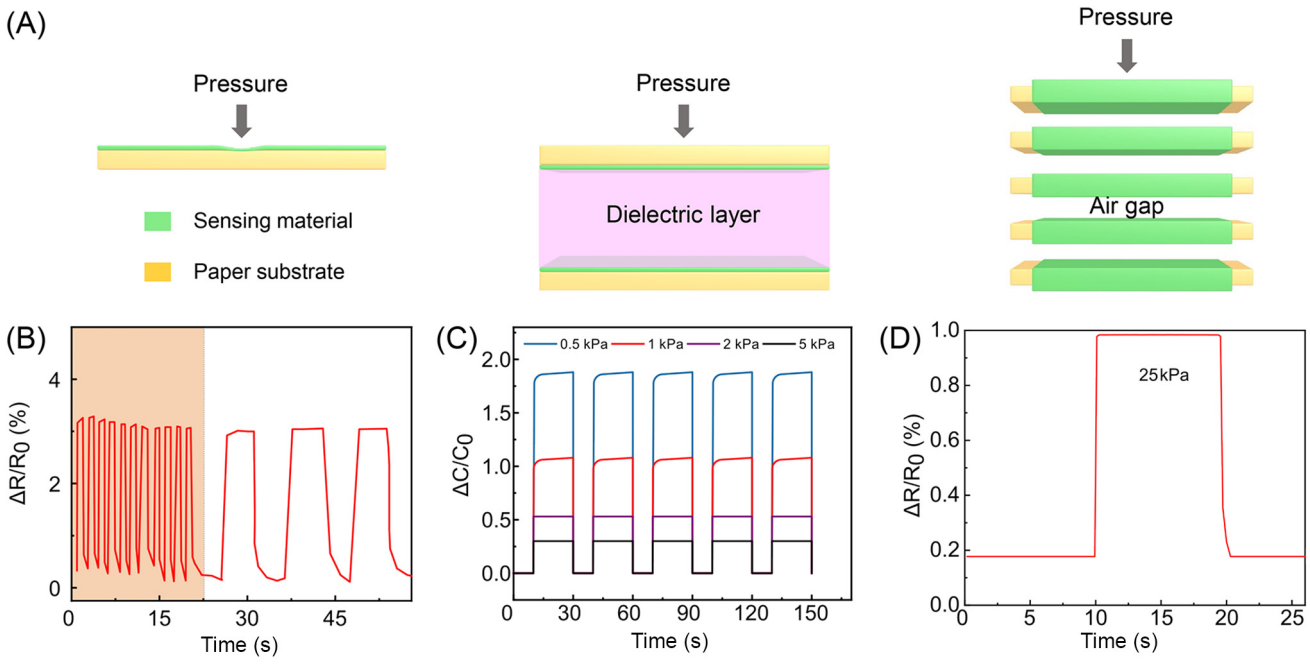

Figure 4. Integrating van der Waals (vdW) materials with paper for pressure sensor applications. (A) Schematic diagrams of pressure sensors with different numbers of layers. (B) Change in the resistance of a graphite-based pressure sensor on paper at different frequencies. Adapted, with permission, from [59]. (C) Change in the capacitance of a graphite-based pressure sensor on paper. Adapted, with permission, from [54]. (D) Change in the resistance of a pressure sensor based on 2D-$SnSe_2$ nanosheet functionalized paper. Adapted, with permission, from [61].

an extensive operating range of 0–20 kPa and a high sensitivity of 17.2 kPa^{-1} of the range of 0–2 kPa [60]. This pressure sensor can detect human physiological activities, including pulsation and respiration.

The rough surface of papers could be considered as a natural microstructure that increases the effective dielectric constant and thus enhances pressure sensitivity during loading. A graphite-covered capacitive pressure sensor was constructed by utilizing the surface roughness of standard printer paper, and its capacitance varied with pressure, as demonstrated in Figure 4C [54]. The microscale roughness and surface curling of the pressure sensor induce interlayer air gaps that contribute to sensitive responses in the low-pressure region. This rough-surface-enabled capacitive pressure sensor presented a pressure sensitivity of 0.62 kPa^{-1} with a low detection limit of 6 Pa and high stability over 1000 bending cycles.

In addition to graphite/graphene, other vdW materials, especially TMDCs, are being explored for their tunable electronic transport. A 2D-$SnSe_2$ nanosheet functionalized paper that operates as a piezoresistive pressure sensor is presented in Figure 4D [61]. Because of the enhanced air gap, the responsivity can be modulated by stacking different numbers of $SnSe_2$-papers, and achieved the highest value of 868% in the broad pressure range of 2–100 kPa. Moreover, this device showed excellent stability over >5000 loading cycles, making it suitable for monitoring human activities such as finger taps, nasal breaths, and wrist pulses.

Strain sensors

The sensitivity of strain sensors depends on the sensing material, operating mechanism, device structure, and other factors. Conventional strain sensors often struggle to meet the demands for wearability and comfort requirements owing to their drawbacks of rigidity and brittleness [62]. Therefore, there is a growing interest in the development of flexible strain sensors. In general, the strain sensitivity, also known as gauge factor (GF), is 2–5 for most metallic materials, ~100 for semiconductor materials, and 1–100 for flexible materials [63,64]. Figure 5A depicts a flexible paper-based strain sensor at tension and compression deformations. When subjected to tension or compression strain, the electrical properties of these devices exhibit a monotonic variation. This strain-dependent sensing mechanism can mostly be attributed to the sliding of active flakes distributed in the sensing area of the device (Figure 5B). The flakes interact through vdW bonding, which results in relatively weak friction, thus allowing the flakes to slide when moderate stress is applied. During compression strain, the flakes compact together to increase flake-to-flake overlap and consequently reduce resistance. By contrast, tension strain forces the flakes to separate, decreasing the overlap and even forming cracks in some locations, thus increasing the resistance of the device.

A paper-based piezoresistive strain sensor was developed with a WS_2 film as the sensing area [65]. As indicated by the current versus voltage characteristics at different uniaxial strains, the resistance increased with tension but decreased with compression strain, yielding a high GF of ~60 (Figure 5C). A graphite-based strain sensor on paper was able to deliver a synchronous electrical response behavior during a repeated strain of 0.2%, demonstrating its promising application in motion detection (Figure 5D) [59].

BP is mechanically robust, and has a **Young's modulus** of 106.4 GPa that can withstand large localized strains without breaking [66], making it an ideal material for flexible strain sensors. A low-cost strain sensor was developed using BP grown on paper as the sensing material and polydimethylsiloxane (PDMS) as a passivation layer to reduce the oxidation of BP [67]. This BP-based device performed over a strain range exceeding 2.5%, and exhibited a GF of 6.1. It also

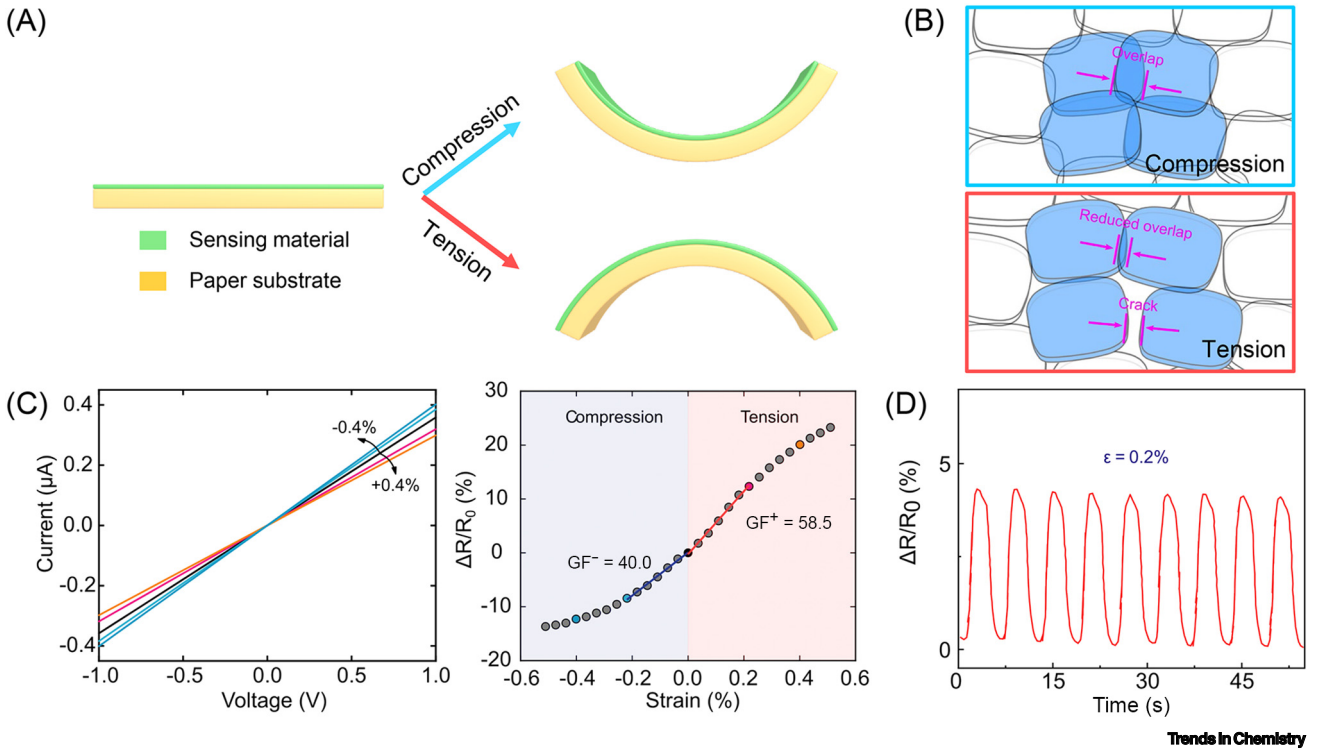

Figure 5. Integrating van der Waals (vdW) materials with paper for strain sensor applications. (A) Illustration of paper-based strain sensors upon compression and tension deformations. (B) Schematic diagrams of the strain-sensing mechanism under compression and tension deformations respectively. (C) Electrical signal changes with applied uniaxial strain for an abrasion-induced deposited WS_2 strain sensor. Adapted, with permission, from [65]. (D) Real-time output signal of a graphite-based strain sensor on paper under repeated bending strain. Adapted, with permission, from [59].

presented strong robustness, and there was no significant change in device performance over 2000 bending cycles. Moreover, the performance of the sensor remained consistent over 98 days, indicating excellent air stability.

Integrating vdW materials with paper for environmental sensing applications

Sensors capable of capturing information in complex environments have seen significant advances over the past few decades. Compared to human perception, these sensors offer higher accuracy to detect subtle ambient changes and broader sensing ranges, and are capable of detecting extreme temperatures up to thousands of degrees [68]. Integrating these sensors with the Internet of Things (IoT) enables data acquisition, analysis, and remote interactive operation of objects. In this section we overview advances in paper-based devices with vdW materials for the detection of ambient temperature, humidity, and gases.

Humidity sensors

Humidity, usually defined as relative humidity (RH), is a non-negligible environmental parameter in daily life and industrial production. Humidity sensors convert moisture per volume into electrical signals, and have applications in healthcare, weather monitoring, agriculture, food storage, and industrial processes [21,69,70]. The humidity sensing mechanism may be elaborated with Lewis acid–base interactions and the Grotthuss chain reaction [71], as shown in Figure 6A. Ambient water molecules are adsorbed to the surface of hydrophilic sensing materials via hydrogen bonding to form a chemisorbed layer. As the concentration of water vapor increases, the hydrogen bonding between adjacent hydroxyl groups facilitates the formation of contiguous multilayer

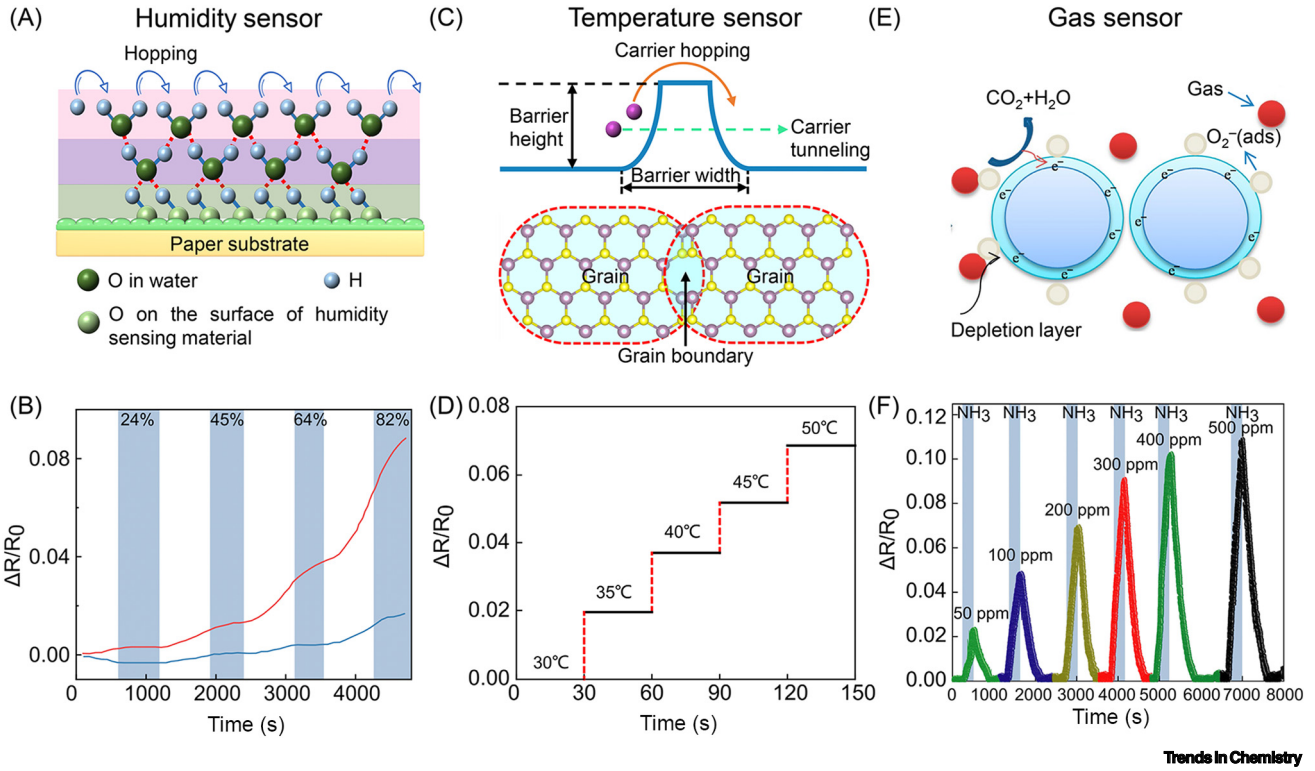

Figure 6. Integrating van der Waals (vdW) materials with paper for environmental sensor applications. (A) Schematic diagram of humidity sensors showing the Grotthuss mechanism. (B) A force and humidity dual-mode sensor based on a polyimide (PI)/paper bilayer structure. Adapted, with permission, from [75]. (C) Schematic diagram of temperature sensors showing the thermal excitation effect of carriers upon exposure to high temperatures. (D) A pencil-paper on-skin temperature sensor. Adapted, with permission, from [44]. (E) Schematic diagram of gas sensors showing the sensing mechanism of an n-type semiconductor for reducing gas. Abbreviation: Ads, adsorbed. Adapted, with permission, from [81]. (F) A room temperature NH_3 gas sensor. Adapted, with permission, from [84].

water by physisorption. In this regime, protons can jump between adjacent water molecules following the Grotthuss mechanism, $H_2O + H_3O^+ \rightarrow H_3O^+ + H_2O$, where H_3O^+ ions act as charge carriers in proton-exchange reactions. Such ionic transport results in a reduction in resistance, thus improving the overall conductivity.

The response of the humidity sensor is generally defined as the ratio of the electrical value of the device at a specific RH to the initial RH. Concerning the negatively responsive resistance humidity sensor, the response can be expressed by two approaches. One is the relative ratio $[(R_0–R_{RH})/R_0 \times 100\%]$ [72], and the other is the absolute ratio (R_0/R_{RH}) [71], where R_0 and R_{RH} are the initial electrical resistance and the electrical resistance at a specific RH, respectively. The sensitivity of the humidity sensor can be represented as the change in electrical value per RH unit, measured as the slope of the response line following a calibrated linear fit [21].

Cellulose fibers can function as a humidity-sensing material because of their hygroscopic character, which allows them to adsorb moisture from the environment, leading to a proportional change in the ionic conductivity of the paper. Inspired by this property, a simple humidity sensor was fabricated using paper as both the sensing material and the substrate, and this presented a response of $>10^3$ over the humidity range of 41.1–91.5% [73]. A paper-based humidity sensor with graphite electrodes can be embedded within a textile procedure mask to monitor respiration pattern and rate [74]. In addition, vdW materials have been extensively integrated with paper to

create highly sensitive humidity sensors. A force and humidity dual-mode sensor was developed based on a polyimide (PI)/paper bilayer structure (Figure 6B) [75]. The PI layer is transformed into a patterned porous graphitic structure by using a direct laser-writing method, allowing it to detect humidity variations. Because of the difference in humidity absorption properties of the PI and paper layers, the sensor bends in a humid environment, causing a change in the resistance of the graphitic pattern.

Temperature sensors

Temperature sensors are designed to convert the temperature of an object or environment into an electrical signal. For common resistive temperature sensors based on semiconductor materials, an increase in temperature causes a decrease in resistance, which is attributed to thermal excitation of the carriers [76], as shown in Figure 6C. Because defects are widely present, free carriers are trapped at the boundaries between adjacent grains, forming a potential barrier Φ that hinders the movement of the carriers. As thermal energy (temperature) increases, the thermally excited carriers can cross the barrier by tunneling and hopping between adjacent grains, resulting in a reduction in resistance. The temperature coefficient of resistance (TCR) is a parameter used to quantify the sensitivity of a temperature sensor, which is expressed as:

$$\mathrm{TCR} = \frac{1}{R}\frac{dR}{dT} = -\frac{\Phi}{kT^2} \quad [1]$$

where T is the temperature, k is the Boltzmann constant, and Φ is the potential barrier [45].

Thermosensitive vdW materials can be integrated with low-cost papers to achieve temperature detection. Graphite is a widely used vdW material for thermal sensing [77,78]. For example, a pencil-paper on-skin temperature sensor was developed, where graphite has high electrical conductivity and paper has low thermal conductivity (Figure 6D) [44]. The device exhibited a clear electrical response as the temperature changed, with a response time of ~90 s and a TCR of –3600 ppm K^{-1}. Semiconducting materials also exhibit strong temperature dependence of resistance. A temperature sensor based on WS_2 nanoplatelets was fabricated on paper and demonstrated a remarkable drop in resistance with increasing temperature [79]. The charge transport in this device was attributed to thermally activated carriers, resulting a TCR ranging from –20 000 ppm K^{-1} to –160 000 ppm K^{-1} and a fast response time of ~0.2 s, demonstrating excellent temperature sensing ability.

Gas sensors

Gas sensors are valuable tools for detecting specific gases because they sense the change in the volume fraction of the target gas and convert this to an electrical signal [80]. Gas adsorption can alter the surface state of a sensing material, leading to a change in the space charge layer and modulating its conductivity (Figure 6E) [81]. For a n-type semiconductor, electrons are the majority charge carriers. Surface states in the semiconductor behave as electron donors or acceptors which exchange with electrons inside the semiconductor to form a space charge layer near the surface. The presence of a reducing gas prompts the desorption of adsorbed oxygen species on the surface, which in turn releases electrons into the material, thereby enhancing its electrical conductivity. In most real situations the gas composition can be complex, and the target gas is surrounded by interfering gases. As a result, a gas sensor must possess high sensitivity and selectivity to identify and categorize the target gas [82,83]. The response and sensitivity parameters of gas sensors are defined in a way that is essentially the same as that for humidity sensors.

Paper substrates are excellent candidates for gas sensing because of their porous structure and high specific surface area. For example, 2D WS_2 nanosheets with sulfur defects were prepared by lithium ion intercalation and exfoliation (Li-2D WS_2) and integrated onto paper as a sensing layer for ammonia (NH_3) gas detection (Figure 6F) [84]. The Li-2D WS_2 nanosheets are p-type, and valence band holes are the majority carriers. When exposed to NH_3 molecules, they accept electrons from NH_3, causing electron–hole recombination, which reduces the concentration of hole carriers, and therefore reduces the conductivity of p-type WS_2. The assembled device on paper eventually presented an excellent response to NH_3 gas, with an average response of ~4.6% at 100 ppm concentration, and the response intensity was more than threefold higher than that of **chemical vapor deposition (CVD)** of 2D WS_2 on a silicon wafer at the same NH_3 concentration. The gas sensitivity of the device did not decay noticeably after 8000 bending cycles, indicating its good stability.

Recently, a highly sensitive and selective NO_2 gas sensor was developed using WS_2 platelets [85]. The WS_2 platelets possess structural continuity, giving higher conductivity for lower detection limits. This sensor delivered a response of ~42% at 0.8 ppm concentration, and established a lower detection limit of ~2 ppb. More importantly, it is highly selective for NO_2 gas, despite the presence of interfering of NH_3 and CO.

Integrating vdW materials with paper for photodetector applications

Paper-based devices with vdW materials also have promising applications in optoelectronics, particularly in photodetectors. Photodetectors convert incident light of various wavelengths into an electrical signal and are essential components in medical imaging, optical communications, security inspections, environmental monitoring, and other fields [86,87].

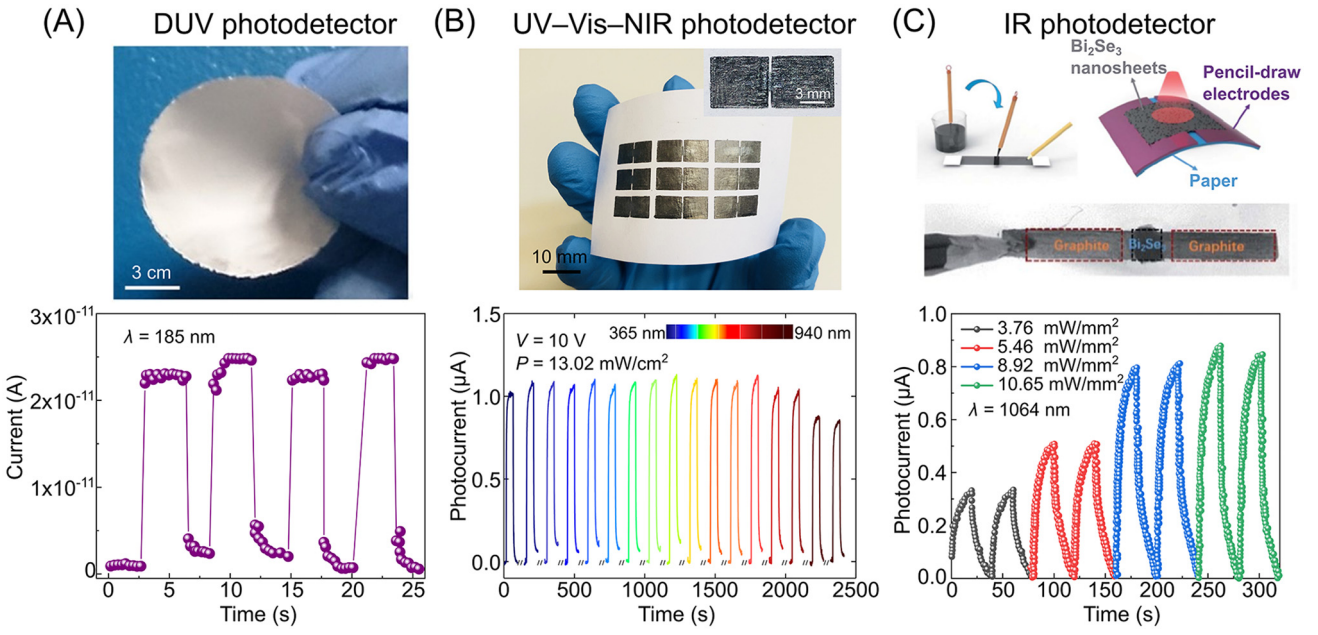

Figure 7. Integrating van der Waals (vdW) materials with paper for photodetector applications. (A) A DUV photodetector based on a BN paper at 185 nm illumination. Adapted, with permission, from [90]. (B) A broadband UV–Vis–NIR photodetector based on a WS_2-on-paper. Adapted, with permission, from [91]. (C) An IR photodetector based on Bi_2Se_3-on-paper at 1064 nm illumination. Adapted, with permission, from [92]. Abbreviations: DUV, deep UV; BN, boron nitride; IR, infrared; NIR, near-IR; Vis, visible.

Compared to commercially available thin-film photodetectors (e.g., silicon photodetectors (Si) and InGaAs photodetectors), the novel photodetectors based on 2D layered TMDCs materials offer appealing features such as physical flexibility, room temperature operating, high photoresponsivity and detectivity, and ultrabroadband spectral response ranging from UV to terahertz frequencies (THz) [88,89]. Responsivity (R) is a typical parameter to evaluate photodetection performance, which is expressed as:

$$R = \frac{I_{ph}}{P \times S_{device}} \quad [2]$$

where P is the incident power intensity, I_{ph} is the photogenerated current, and S_{device} is the active channel area of the device upon illumination [86].

Recent studies have reported the fabrication of flexible paper-based photodetectors with distinct detection ranges using various vdW materials. For instance, a flexible solar-blind photodetector was fabricated using a hexagonal boron nitride (*h*-BN) paper supported with cellulose nanofibers, and achieved excellent photodetection at 185 nm illumination with a responsivity of ~0.05 mA W^{-1} and a short response time of 0.267 s at 10 V (Figure 7A) [90]. A broad-band WS_2 photodetector on paper was also reported, as shown in Figure 7B [91]. It could detect incident light ranging from 365 nm (UV) to 940 nm (near-IR), with a high responsivity of ~270 mA W^{-1} (at 35 V). Given these advantageous properties, these paper-based photodetectors have promising applications as optical detector elements in spectrometers. In addition, an IR photodetector was developed using liquid-exfoliated Bi_2Se_3 nanosheets, and exhibited a responsivity of 26.69 μA W^{-1} with excellent flexibility and stability in the bending state upon 1064 nm illumination at 5 V voltage (Figure 7C) [92].

To enhance photoelectrical performance further, a combination of two or more materials is highly recommended because it increases light absorbance and thus increases the responsivity. These combinations include metal nanoparticles-MoS_2 [93], WSe_2-polyaniline (PANi) [94], WSe_2/graphite [95], ZnS-MoS_2 [96], and graphite/ZnO-WS_2 [97] hybrid compositions. The properties can be engineered by constructing vdW heterostructures by in-plane or vertical stacking [98]. For instance, a MoS_2/WSe_2 heterostructure was synthesized as active material to fabricate a paper-based photodetector [99]. Electron–hole pairs are generated in both MoS_2 and WSe_2 upon illumination. The electrons diffuse from the conduction band of WSe_2 to the conduction band of MoS_2, and are eventually collected on the electrode. The interface formed between n-MoS_2 and p-WSe_2 could help to reduce the probability of trapping the photogenerated carrier. This MoS_2/WSe_2 photodetector presented excellent performance, with a high photoresponsivity of about 124 mA W^{-1} and an external quantum efficiency of 23.1%. In addition, a TiS_3–MoS_2 heterostructure was built by placing MoS_2 on top of TiS_3 [100]. The formation of a type II band offset in the TiS_3–MoS_2 heterojunction could promote the effective separation of electrons and holes. Therefore, the TiS_3–MoS_2 photodetector delivered an exceptional optoelectronic performance with a faster response time (0.96 s) and higher on–off ratio (1.82) relative to the individual MoS_2 and TiS_3 photodetectors.

Concluding remarks

Over the past decade we have witnessed remarkable advances in the field of flexible electronics and optoelectronics, particularly through the integration of paper-based devices with various vdW materials. Cellulose paper offers numerous advantages, such as flexibility, biodegradability, and biocompatibility, as well as a large specific surface area and abundant surface functional

Outstanding questions

Can we develop new strategies to extensively integrate vdW materials with paper? Can we combine the current established industry roll-to-roll methodology with paper electronics based on vdW materials?

How can we establish vdW heterostructures on paper? vdW heterostructures integrated on silicon wafers are reported to deliver numerous novel properties, but there have been few reports of their construction on paper substrates.

Can we refine papermaking technology to diminish the impurities in vdW functional materials?

Can we leverage the properties of origami and kirigami to enhance the performance and diversity of paper electronics based on vdW materials?

Can we construct sophisticated devices with high spatial resolution and low energy consumption by employing fibrous-textured paper?

Can we encapsulate the paper-based devices without sacrificing biodegradability?

Can we further engineer the miniaturization and integratability of paper-based electronic systems to achieve multimodal all-in-one sensing and wireless communication capabilities?

Can we utilize artificial intelligence to promote innovative vdW heterostructures and device topology in the field of paper electronics?

groups. These characteristics make paper an ideal eco-friendly, low-cost alternative to traditional silicon, glass, and synthetic polymer substrates for wearable devices. The weak vdW interactions between the individual layers of 2D materials allow the creation of variety of 2D vdW materials including semimetals, semiconductors, superconductors, and insulators. These materials boast exceptional mechanical, optical, and electrical properties, making them well suited for integration with paper-based devices. By incorporating these vdW materials onto paper, devices can be developed to sense various factors, including deformation, humidity, temperature, and gas. The numerous potential applications of paper-based devices with vdW materials highlight the promising future of flexible electronics and optoelectronics.

Despite significant progress, numerous challenges and issues must be addressed before large-scale, mature applications can be realized in the realm of paper-based electronics and optoelectronics (see Outstanding questions). During the standard papermaking process, fillers are introduced that potentially contaminate vdW functional materials and hinder device performance. In addition to composition, the dimension and structure of the paper fibers play significant roles in device performance [101]. As a result, it is recommended to develop customized papermaking processes specifically for electronics and optoelectronics, as opposed to ordinary writing paper. Another considerable challenge in device preparation is the inherently high porosity and surface roughness of paper because these factors can increase energy consumption and decrease pattern resolution. Furthermore, advanced encapsulation processes for paper-based devices are crucial to ensure their reproducibility and durability by diminishing aging effects under various environment conditions such as irradiation, humidity, and ambient oxidation [102]. In addition, biodegradability should not be compromised when sealing them from external interference. Moreover, the development of highly integrated and miniaturized paper-based electronic systems is eagerly anticipated. One feasible approach is to establish multimodal sensing using a single material by exploiting the unique advantages of semiconducting vdW materials such as WS_2. To advance this promising field, researchers from across different disciplines are encouraged to collaborate and contribute their expertise. Given the growing investment in novel synthesis and manufacturing technologies, device performances could be further improved to meet the future demands of cost-effective, eco-friendly, and wearable electronics and optoelectronics.

Acknowledgments

We acknowledge funding by the European Research Council (ERC) through project 2D-TOPSENSE (GA 755655), the EU Horizon 2020 Research and Innovation program (Graphene Core2-Graphene-based disruptive technologies, grant agreement 881603, and Graphene Core3-Graphene-based disruptive technologies, 956813), EU FLAG-ERA program through project To2Dox (JTC-2019-009), the Comunidad de Madrid through the CAIRO-CM project (Y2020/NMT-6661), and the Spanish Ministry of Science and Innovation (TED2021-132267B-I00 and PID2020-115566RB-I00). Financial support from the National Natural Science Foundation of China (NSFC; 62011530438 and 61704129) is also acknowledged. This work was supported in part by the Key Research and Development Program of Shaanxi (2021KW-02), Fundamental Research Funds for the Central Universities (QTZX23026), and the fund of the State Key Laboratory of Solidification Processing at Northwestern Polytechnic University (SKLSP201612).

Declaration of interests

No interests are declared.

References

1. Jung, Y.H. *et al.* (2015) High-performance green flexible electronics based on biodegradable cellulose nanofibril paper. *Nat. Commun.* 6, 7170
2. Nandy, S. *et al.* (2021) Cellulose: a contribution for the zero e-waste challenge. *Adv. Mater. Technol.* 6, 2000994
3. Martins, R. *et al.* (2018) Papertronics: multigate paper transistor for multifunction applications. *Appl. Mater. Today* 12, 402–414
4. Tobjörk, D. and Österbacka, R. (2011) Paper electronics. *Adv. Mater.* 23, 1935–1961
5. Fu, Q. *et al.* (2021) Emerging cellulose-derived materials: a promising platform for the design of flexible wearable sensors toward health and environment monitoring. *Mater. Chem. Front.* 5, 2051–2091
6. Zhu, P. *et al.* (2021) Electrostatic self-assembly enabled flexible paper-based humidity sensor with high sensitivity and superior durability. *Chem. Eng. J.* 404, 127105

7. Li, S. *et al.* (2019) All-in-one iontronic sensing paper. *Adv. Funct. Mater.* 29, 1807343
8. Choi, K.H. *et al.* (2016) All-inkjet-printed, solid-state flexible supercapacitors on paper. *Energy Environ. Sci.* 9, 2812–2821
9. Martins, R. *et al.* (2011) Complementary metal oxide semiconductor technology with and on paper. *Adv. Mater.* 23, 4491–4496
10. Hu, L. *et al.* (2013) Transparent and conductive paper from nanocellulose fibers. *Energy Environ. Sci.* 6, 513–518
11. Park, J.H. *et al.* (2017) Dry writing of highly conductive electrodes on papers by using silver nanoparticle-graphene hybrid pencils. *Nanoscale* 9, 555–561
12. Novoselov, K.S. *et al.* (2005) Two-dimensional gas of massless Dirac fermions in graphene. *Nature* 438, 197–200
13. Frisenda, R. *et al.* (2020) Naturally occurring van der Waals materials. *npj 2D Mater. Appl.* 4, 38
14. Fortunato, E. *et al.* (2008) High-performance flexible hybrid field-effect transistors based on cellulose fiber paper. *IEEE Electron Device Lett.* 29, 988–990
15. Ajayan, P. *et al.* (2016) Two-dimensional van der Waals materials. *Phys. Today* 69, 38–44
16. Liu, Y. *et al.* (2016) Van der Waals heterostructures and devices. *Nat. Rev. Mater.* 1, 16042
17. Li, X. *et al.* (2009) Large-area synthesis of high-quality and uniform graphene films on copper foils. *Science* 324, 1312–1314
18. Conti, S. *et al.* (2023) Printed transistors made of 2D material-based inks. *Nat. Rev. Mater.* 8, 651–667
19. Tang, Q. *et al.* (2020) Recent progresses on paper-based triboelectric nanogenerator for portable self-powered sensing systems. *EcoMat* 2, 12060
20. Tai, H. *et al.* (2020) Paper-based sensors for gas, humidity, and strain detections: a review. *ACS Appl. Mater. Interfaces* 12, 31037–31053
21. Duan, Z. *et al.* (2021) Recent advances in humidity sensors for human body related humidity detection. *J. Mater. Chem. C* 9, 14963–14980
22. Liu, Y. *et al.* (2019) Van der Waals integration before and beyond two-dimensional materials. *Nature* 567, 323–333
23. Zhang, X. *et al.* (2020) Two-dimensional GeTe: air stability and photocatalytic performance for hydrogen evolution. *ACS Appl. Mater. Interfaces* 12, 37108–37115
24. Zhang, F. *et al.* (2020) Few-layer and large flake size borophene: preparation with solvothermal-assisted liquid phase exfoliation. *RSC Adv.* 10, 27532–27537
25. Nagyte, V. *et al.* (2020) Raman fingerprints of graphene produced by anodic electrochemical exfoliation. *Nano Lett.* 20, 3411–3419
26. Velický, M. *et al.* (2017) Exfoliation of natural van der Waals heterostructures to a single unit cell thickness. *Nat. Commun.* 8, 14410
27. Song, Q.J. *et al.* (2016) Physical origin of Davydov splitting and resonant Raman spectroscopy of Davydov components in multilayer $MoTe_2$. *Phys. Rev. B* 93, 115409
28. Zhang, W. *et al.* (2021) Integrating van der Waals materials on paper substrates for electrical and optical applications. *Appl. Mater. Today* 23, 101012
29. Jang, S. *et al.* (2017) Simple and rapid fabrication of pencil-on-paper triboelectric nanogenerators with enhanced electrical performance. *Nanoscale* 9, 13034–13041
30. Yao, B. *et al.* (2013) Paper-based solid-state supercapacitors with pencil-drawing graphite/polyaniline networks hybrid electrodes. *Nano Energy* 2, 1071–1078
31. Liao, X. *et al.* (2015) Flexible and highly sensitive strain sensors fabricated by pencil drawn for wearable monitor. *Adv. Funct. Mater.* 25, 2395–2401
32. Acerce, M. *et al.* (2015) Metallic 1T phase MoS_2 nanosheets as supercapacitor electrode materials. *Nat. Nanotechnol.* 10, 313–318
33. Wang, Y.H. *et al.* (2017) Recent advances in transition-metal dichalcogenides based electrochemical biosensors: a review. *Biosens. Bioelectron.* 97, 305–316
34. Azpeitia, J. *et al.* (2021) Integrating superconducting van der Waals materials on paper substrates. *Mater. Adv.* 2, 3274–3281
35. Conti, S. *et al.* (2020) Low-voltage 2D materials-based printed field-effect transistors for integrated digital and analog electronics on paper. *Nat. Commun.* 11, 3566
36. Wu, M. *et al.* (2021) Synthesis of two-dimensional transition metal dichalcogenides for electronics and optoelectronics. *InfoMat* 3, 362–396
37. Hu, G. *et al.* (2018) Functional inks and printing of two-dimensional materials. *Chem. Soc. Rev.* 47, 3265–3300
38. McManus, D. *et al.* (2017) Water-based and biocompatible 2D crystal inks for all-inkjet-printed heterostructures. *Nat. Nanotechnol.* 12, 343–350
39. Mampallil, D. and Burak, H. (2018) A review on suppression and utilization of the coffee-ring effect. *Adv. Colloid Interf. Sci.* 252, 38–54
40. Say, M.G. *et al.* (2020) Spray-coated paper supercapacitors. *npj Flex. Electron.* 4, 14
41. Kim, Y.D. and Hone, J. (2017) Screen printing of 2D semiconductors. *Nature* 544, 167–168
42. Tang, X. and Yan, X. (2017) Dip-coating for fibrous materials: mechanism, methods and applications. *J. Sol-Gel Sci. Technol.* 81, 378–404
43. Liu, H. *et al.* (2017) Flexible and degradable paper-based strain sensor with low cost. *ACS Sustain. Chem. Eng.* 5, 10538–10543
44. Xu, Y. *et al.* (2020) Pencil-paper on-skin electronics. *Proc. Natl. Acad. Sci. U. S. A.* 117, 18292–18301
45. Dinh, T. *et al.* (2015) Graphite on paper as material for sensitive thermoresistive sensors. *J. Mater. Chem. C* 3, 8776–8779
46. Nutting, D. *et al.* (2020) Heterostructures formed through abraded van der Waals materials. *Nat. Commun.* 11, 3047
47. Le, T.-S.D. *et al.* (2022) Recent advances in laser-induced graphene: mechanism, fabrication, properties, and applications in flexible electronics. *Adv. Funct. Mater.* 32, 2205158
48. Kulyk, B. *et al.* (2021) Laser-induced graphene from paper for mechanical sensing. *ACS Appl. Mater. Interfaces* 13, 10210–10221
49. Kulyk, B. *et al.* (2022) Laser-induced graphene from paper for non-enzymatic uric acid electrochemical sensing in urine. *Carbon* 197, 253–263
50. Pedro, P.I. *et al.* (2022) Sustainable carbon sources for green laser-induced graphene: a perspective on fundamental principles, applications, and challenges. *Appl. Phys. Rev.* 9, 041305
51. Kokkinos, C. *et al.* (2018) Paper-based device with a sputtered tin-film electrode for the voltammetric determination of Cd(II) and Zn(II). *Sensors Actuators B Chem.* 260, 223–226
52. Li, H. *et al.* (2020) Flexible ultraviolet photodetector based ZnO film sputtered on paper. *Vacuum* 172, 109089
53. Gao, L. *et al.* (2019) All paper-based flexible and wearable piezoresistive pressure sensor. *ACS Appl. Mater. Interfaces* 11, 25034–25042
54. Lee, K. *et al.* (2017) Rough-surface-enabled capacitive pressure sensors with 3D touch capability. *Small* 13, 38–44
55. Kim, Y.G. *et al.* (2022) Piezoelectric strain sensor with high sensitivity and high stretchability based on kirigami design cutting. *npj Flex. Electron* 6, 52
56. Souri, H. *et al.* (2020) Wearable and stretchable strain sensors: materials, sensing mechanisms, and applications. *Adv. Intell. Syst.* 2, 2000039
57. Zhu, M. *et al.* (2021) A review of strain sensors based on two-dimensional molybdenum disulfide. *J. Mater. Chem. C* 9, 9083–9101
58. Qi, X. *et al.* (2020) Mulberry paper-based graphene strain sensor for wearable electronics with high mechanical strength. *Sens. Actuators A Phys.* 301, 111697
59. Liu, H. *et al.* (2022) Paper-based flexible strain and pressure sensor with enhanced mechanical strength and superhydrophobicity that can work under water. *J. Mater. Chem. C* 10, 3908–3918
60. Tao, L.Q. *et al.* (2017) Graphene-paper pressure sensor for detecting human motions. *ACS Nano* 11, 8790–8795
61. Tannarana, M. *et al.* (2020) 2D-$SnSe_2$ nanosheet functionalized piezo-resistive flexible sensor for pressure and human breath monitoring. *ACS Sustain. Chem. Eng.* 8, 7741–7749

62. Seyedin, S. *et al.* (2019) Textile strain sensors: a review of the fabrication technologies, performance evaluation and applications. *Mater. Horiz.* 6, 219–249
63. Xing, Y. *et al.* (2007) Measurement and simulation of carbon nanotube's piezoresistance property by a micro/nano combined structure. *Indian J. Pure Appl. Phys.* 45, 282–286
64. Fiorillo, A.S. *et al.* (2018) Theory, technology and applications of piezoresistive sensors: a review. *Sens. Actuators A Phys.* 281, 156–175
65. Zhang, W. *et al.* (2021) Paper-supported WS_2 strain gauges. *Sens. Actuators A Phys.* 332, 113204
66. Jiang, J.W. and Park, H.S. (2014) Mechanical properties of single-layer black phosphorus. *J. Phys. D. Appl. Phys.* 47, 14–17
67. Selamneni, V. *et al.* (2020) Highly air-stabilized black phosphorus on disposable paper substrate as a tunnelling effect-based highly sensitive piezoresistive strain sensor. *Med. Devices Sens.* 3, 10099
68. Chen, J. *et al.* (2021) Recent progress in essential functions of soft electronic skin. *Adv. Funct. Mater.* 31, 2104686
69. Jung, C. *et al.* (2022) Disordered-nanoparticle-based etalon for ultrafast humidity-responsive colorimetric sensors and anti-counterfeiting displays. *Sci. Adv.* 8, 8598
70. Duan, Z. *et al.* (2021) Daily writing carbon ink: novel application on humidity sensor with wide detection range, low detection limit and high detection resolution. *Sensors Actuators B Chem.* 339, 129884
71. Sun, L. *et al.* (2018) Effective use of biomass ash as an ultra-high humidity sensor. *J. Mater. Sci. Mater. Electron.* 29, 18502–18510
72. Wang, Y. *et al.* (2020) Flexible and transparent cellulose-based ionic film as a humidity sensor. *ACS Appl. Mater. Interfaces* 12, 7631–7638
73. Duan, Z. *et al.* (2019) Facile, flexible, cost-saving, and environment-friendly paper-based humidity sensor for multifunctional applications. *ACS Appl. Mater. Interfaces* 11, 21840–21849
74. Güder, F. *et al.* (2016) Paper-based electrical respiration sensor. *Angew. Chem. Int. Ed.* 55, 5727–5732
75. Luo, J. *et al.* (2018) Force and humidity dual sensors fabricated by laser writing on polyimide/paper bilayer structure for pulse and respiration monitoring. *J. Mater. Chem. C* 6, 4727–4736
76. Kuzubasoglu, B.A. and Bahadir, S.K. (2020) Flexible temperature sensors: a review. *Sens. Actuators A Phys.* 315, 112282
77. Paquin, F. *et al.* (2015) Multi-phase semicrystalline microstructures drive exciton dissociation in neat plastic semiconductors. *J. Mater. Chem. C* 3, 10715–10722
78. Huang, Y. *et al.* (2018) High-resolution flexible temperature sensor based graphite-filled polyethylene oxide and polyvinylidene fluoride composites for body temperature monitoring. *Sens. Actuators A Phys.* 278, 1–10
79. Lee, M. *et al.* (2020) Drawing WS_2 thermal sensors on paper substrates. *Nanoscale* 12, 22091–22096
80. Dai, J. *et al.* (2020) Printed gas sensors. *Chem. Soc. Rev.* 49, 1756–1789
81. Nikolic, M.V. *et al.* (2020) Semiconductor gas sensors: materials, technology, design, and application. *Sensors* 20, 6694
82. Peña, Á. *et al.* (2023) Optimization of multilayer graphene-based gas sensors by ultraviolet photoactivation. *Appl. Surf. Sci.* 610, 155393
83. Li, Z. *et al.* (2019) Advances in designs and mechanisms of semiconducting metal oxide nanostructures for high-precision gas sensors operated at room temperature. *Mater. Horiz.* 6, 470–506
84. Qin, Z. *et al.* (2022) Development of flexible paper substrate sensor based on 2D WS_2 with S defects for room-temperature NH_3 gas sensing. *Appl. Surf. Sci.* 573, 151535
85. Matatagui, D. *et al.* (2022) Eco-friendly disposable WS_2 paper sensor for sub-ppm NO_2 detection at room temperature. *Nanomaterials* 12, 1213
86. Mazaheri, A. *et al.* (2020) MoS_2-on-paper optoelectronics: drawing photodetectors with van der Waals semiconductors beyond graphite. *Nanoscale* 12, 19068–19074
87. Cai, S. *et al.* (2019) Materials and designs for wearable photodetectors. *Adv. Mater.* 31, 1808138
88. Quereda, J. *et al.* (2022) Scalable and low-cost fabrication of flexible WS_2 photodetectors on polycarbonate. *npj Flex. Electron.* 6, 23
89. Qiu, Q. and Huang, Z. (2021) Photodetectors of 2D materials from ultraviolet to terahertz waves. *Adv. Mater.* 33, 2008126
90. Lin, C.H. *et al.* (2018) A flexible solar-blind 2D boron nitride nanopaper-based photodetector with high thermal resistance. *npj 2D Mater. Appl.* 2, 23
91. Zhang, W. *et al.* (2023) Solvent-free fabrication of broadband WS_2 photodetectors on paper. *Opto-Electron. Adv.* 6, 220101
92. Liu, S. *et al.* (2020) Two-dimensional Bi_2Se_3 nanosheet based flexible infrared photodetector with pencil-drawn graphite electrodes on paper. *Nanoscale Adv.* 2, 906–912
93. Selamneni, V. *et al.* (2021) MoS_2/Paper decorated with metal nanoparticles (Au, Pt, and Pd) based plasmonic-enhanced broadband (visible-NIR) flexible photodetectors. *Adv. Mater. Interfaces* 8, 2001988
94. Kannichankandy, D. *et al.* (2020) Paper based organic–inorganic hybrid photodetector for visible light detection. *Appl. Surf. Sci.* 524, 146589
95. Pataniya, P.M. and Sumesh, C.K. (2020) Low cost and flexible photodetector based on WSe_2 nanosheets/graphite heterostructure. *Synth. Met.* 265, 116400
96. Gomathi, P.T. *et al.* (2017) Large-area, flexible broadband photodetector based on ZnS–MoS_2 hybrid on paper substrate. *Adv. Funct. Mater.* 27, 1701611
97. Patel, M. *et al.* (2022) Flexible photodetector based on graphite/ZnO–WS_2 nanohybrids on paper. *J. Mater. Sci. Mater. Electron.* 33, 13771–13781
98. Geim, A.K. and Grigorieva, I.V. (2013) Van der Waals heterostructures. *Nature* 499, 419–425
99. Pataniya, P.M. *et al.* (2021) MoS_2/WSe_2 nanohybrids for flexible paper-based photodetectors. *Nanotechnology* 32, 315709
100. Mahmoodi, E. *et al.* (2022) Paper-based broadband flexible photodetectors with van der Waals materials. *Sci. Rep.* 12, 12585
101. Pereira, L. *et al.* (2014) The influence of fibril composition and dimension on the performance of paper gated oxide transistors. *Nanotechnology* 25, 094007
102. Duan, Z. *et al.* (2021) Integrated cross-section interface engineering and surface encapsulating strategy: a high-response, waterproof, and low-cost paper-based bending strain sensor. *J. Mater. Chem. C* 9, 14003–14011